

Single Nucleotide Variants (SNVs) Define Senescence-Accelerated SAMP8 Mice, a Model of a Geriatric Condition

Fabien Delerue^a, Geoff Sjollem^b, Belinda Whittle^b, Sarah Krüger^a, Dan Andrews^b and Jürgen Götz^{a,c,*}

^a*Brain and Mind Research Institute, University of Sydney, Camperdown, NSW, Australia*

^b*Australian Phenomics Facility (APF), John Curtin School of Medical Research, Australian National University, Acton, ACT, Australia*

^c*Centre for Ageing Dementia Research (CADR) at the Queensland Brain Institute (QBI), The University of Queensland, Brisbane, QLD, Australia*

Handling Associate Editor: Michal Novak

Accepted 20 March 2013

Abstract. One of the major challenges in neurodegenerative research is modeling systemic aging. Here, senescence-accelerated mice such as the multigenic SAMP8 (senescence accelerated prone 8) mice are useful as they are characterized by an early manifestation of senescence that includes a shortened lifespan and impaired brain and immune functions. While SAMP8 mice are widely used tools to address aging and neurodegenerative conditions such as Alzheimer's disease (AD), the underlying gene mutations are not known. To make the SAMP8 strain a more versatile and useful research tool, we performed exome sequencing, using SAMR1 (senescence accelerated mouse resistant 1) mice as controls. We identified 51 SNVs (single nucleotide variants) that discriminate SAMP8 from SAMR1 mice. Using the prediction tool Polyphen2, we were able to subdivide the SNVs into four categories: splice variants, probably damaging, possibly damaging, and benign. Of these genes, a significant fraction is predicted to be expressed in the brain. Our data present these genes for a more detailed analysis in aging and neurodegeneration studies. They underscore the usefulness of SAMP8 mice as an animal model to study fundamental mechanisms of both aging and the pathogenesis of AD.

Keywords: Alzheimer's disease, exome sequencing, mouse, senescence, sequence nucleotide variants

INTRODUCTION

Aging is the major risk factor for a plethora of human diseases. This includes Alzheimer's disease (AD), a neurodegenerative disorder that is characterized by a progressive decline in memory and other cognitive

functions, leading to dementia [1]. To better understand the underlying pathogenic mechanisms and to develop targeted therapies, a host of transgenic animal models has been developed that reproduce amyloid plaques and neurofibrillary tangles, the two brain lesions characteristic of the human condition [2]. A prerequisite for developing these lesions in mice has been the transgenic expression of the tau-encoding *MAPT* or the amyloid- β protein precursor ($A\beta$ PP)-encoding *A β PP* gene together with pathogenic mutations that are

*Correspondence to: Jürgen Götz, Centre for Ageing Dementia Research (CADR), Queensland Brain Institute (QBI), The University of Queensland, Brisbane, QLD 4072, Australia. Tel.: +61 7 3346 6329; Fax: +61 7 3346 6301; E-mail: j.götz@uq.edu.au.

present in early-onset familial cases. The vast majority of AD cases, however, are of late onset and hence, transgenic models do not faithfully model these sporadic cases. Here, senescence-accelerated mice such as the SAMP8 (senescence accelerated prone 8) strain might be useful, as these mice display many features known to occur early in the pathogenesis of AD, such as increased oxidative stress and memory impairment [3]. SAMP8 mice are therefore an excellent model for studying the earliest neurodegenerative changes associated with AD, providing a more encompassing picture of human disease, a syndrome that is triggered by a combination of age-related events [4].

Together with a series of related senescence-accelerated mice, the SAMP8 strain was established around 1975 by conventional inbreeding of AKR/J-derived mice that displayed features of accelerated aging such as hair loss, reduced activity, shortened life expectancy, lordokyphosis (increased curvature of the spine), and periophthalmic (around the eye) problems [5]. Littermates of mice that did not show a senescence-associated phenotype were also inbred, and senescence-resistant, longer-lived SAMR mice were obtained of which SAMR1 (senescence accelerated mouse resistant 1) mice are commercially available. SAMP strains exhibit an early onset of age-related decline in the peripheral immunity such as thymic involution, loss of CD4(+) T cells, impaired helper T cell function, decreased antibody-forming capacity, dysfunction of antigen-presenting cells, decreased natural killer activity, increased auto-antibodies, and susceptibility to viral infection [6].

SAMP8 mice have been extensively analyzed for cognitive functions [7]. Impairment of spatial memory is initiated at the age of four months, as shown by using various forms of water and radial arm mazes [8–10]. By employing the more sensitive radial arm water maze, impairments in spatial learning became evident as early as three months of age [11]. In measuring associative memories, fear conditioning or passive avoidance tasks are widely used [12, 13]. In SAMP8 mice, while associative learning as assessed in the fear conditioning-paradigm is not affected, both passive and active avoidance (i.e., learning to escape the environment in which the aversive stimulus has been received) are affected, with an age of onset as early as two months [14, 15].

SAMP8 mice are neuropathologically characterized by oxidative changes similar to those found in the AD brain [16]. For example, key enzymes that detoxify reactive oxygen species such as MnSOD, catalase or glutathione peroxidase are all decreased in SAMP8

compared to SAMR1 mice [17–19]. Increased lipid peroxidation and carbonyl damage is present as early as 2 months of age [20]. Furthermore, SAMP8 mice have an impaired glucose metabolism [21], and reveal age-dependent reductions of various receptors including for NMDA [22]. Because in the AD brain, deposition of A β leads to plaque formation and that of the microtubule-associated protein tau to tangle formation, these two processes have been extensively analyzed in SAMP8 mice [23]. Tau was found to be hyperphosphorylated using a small set of phosphorylation site-specific antibodies, but tau filament formation and tangle formation has not been reported indicating that the SAMP8 mice present with an early rather than a more advanced tau pathology [23]. In phosphorylating tau and causing its aggregation [24], studies in SAMP8 mice suggest a role for the kinases GSK3 and Cdk5 [25]. Staining with A β -specific antibodies suggested A β deposition in the mice [26, 27]; however because different from the human sequence of A β PP, the murine protein lacks the amino acids that are required to generate A β in the first place, these deposits have been termed ‘A β -like’ [26]. For A β PP, age-related increases have been reported, both at the protein and mRNA level [28–30]. Finally, a glial pathology characterizes the aging brain and in particular, the AD brain, and not surprisingly, SAMP8 mice present with a marked astro- and microgliosis [30, 31]. These findings present SAMP8 mice as a suitable model for aging dementia, thereby complementing the existing transgenic mouse models.

However, a major drawback in making the best use of senescence-accelerated mice is that their phenotype is multigenic and that the underlying gene mutations are not known. Therefore, we obtained SAMP8 mice from a commercial breeder and phenotypically characterized them. To make the SAMP8 model more suitable for geriatric studies, we performed massively parallel exome sequencing [32]. By applying this method to SAMP8 and SAMR1 mice, we were able to identify 51 SAMP8-specific single nucleotide variants (SNVs), followed by a Polyphen2 analysis that allows phenotype predictions.

MATERIALS AND METHODS

Animals

SAMP8/TaHsd (in short: SAMP8) and SAMR1/TaHsd (in short: SAMR1) mice were obtained from Harlan Laboratories UK Ltd. They were rederived by

embryo transfer followed by expansion of a colony in the SPF unit of our institute's animal facility. Animal experimentation was approved by the Animal Ethics Committee (AEC) of the University of Sydney (approval number K00/1-2009/3/4914).

Phenotypic analysis and histology

The weight of the mice was monitored on a weekly basis. Immunohistochemical staining for glial fibrillar acidic protein (GFAP) was done on 3 μ m sections of paraformaldehyde-fixed and paraffin-embedded brain tissue of 6 month-old mice as described [33]. More specifically, brains were fixed in paraformaldehyde and embedded in paraffin using an Excalibur tissue processor (Thermo). Antigen retrieval was done in a temperature- and pressure-controlled microwave system (Milestone) in Tris/EDTA pH 9.0 for 7 min at 120°C, followed by cooling under running tap water for 10 min. Primary antibody anti-GFAP (monoclonal IgG, Sigma, #63893) was diluted 1:100 in blocking buffer (heat inactivated 3% normal goat serum, 2% BSA, 0.1% Tween-20 in 1 \times PBS) and incubated overnight at 4°C. After three washes in 1 \times PBS, the sections were incubated with an Alexa-coupled secondary antibody (Invitrogen, #A-11001) for 1 h at room temperature, followed by three washes in 1 \times PBS. The sections were then mounted in Fluoromount medium (Sigma # F4680) and digital images taken with a BX51 fluorescent microscope (Olympus).

Exome sequencing

Exome enriched, paired end libraries were prepared from genomic DNA of two SAMP8 and two SAMR1 mice following the protocol 'SureSelect Target Enrichment System for Illumina Paired-End Multiplexed Sequencing library' (v1.1.1, November 2010, Agilent). The Illumina Paired-end genomic DNA sample prep kit (PE-102-1001, Illumina) was used for preparing the libraries including end repair, A-tailing, and ligation of the Illumina adaptors. For capture, SureSelect Mouse exome baits (G7550, Agilent) were used to enrich for the mouse exome. Each sample was prepared with an index in an amplification step following capture using the Illumina multiplexing sample preparation oligo-nucleotide kit (PE-400-1001, Illumina). Enriched sample libraries were pooled in equimolar batches of three and each batch run as 100 bp paired end libraries on the Illumina HiSeq 2000 sequencer.

Data analysis

Sequence reads were mapped to the NCBIM37 assembly of the reference mouse genome using Burrows-Wheeler Aligner (<http://bio-bwa.sourceforge.net>) [34]. Untrimmed reads were aligned allowing a maximum of two sequence mismatches and were discarded where they aligned to the genome more than once. Sequence variants were identified with SAMtools (<http://samtools.sourceforge.net>) [35] and annotated using Annovar (<http://www.openbioinformatics.org>) [36]. A version of PolyPhen2 (<http://genetics.bwh.harvard.edu/pph2>) [37], adapted for the mouse, was utilized for the calculation of the variant effect.

Validation of single nucleotide variants

SNVs identified by Next Generation Sequencing were validated using the Amplifluor SNP genotyping system (Chemicon, Millipore). Assays were designed to each SNV of interest and validated against a set of Samp8 and SamR1 mice. Primer sequences for each SNV that has been assayed can be found in the Supplementary Table 1 (available online: <http://dx.doi.org/10.3233/JAD-130089>).

RESULTS

Phenotypic characterization of SAMP8 mice

To phenotypically characterize SAMP8 mice and differentiate them from SAMR1 mice, we determined the lifespan of both strains. According to Harlan from whom we had obtained the mice, the median survival time of SAMP8 mice is 12.1 months whereas SAMR1 mice have a median survival time of 18.9 months. Others reported a mean lifespan of 9.7 months for SAMP mice (not specifying the sub-strain) and 16.3 months for SAMR mice, while standard inbred mouse strains (such as C57Bl/6) have a life expectancy in the order of 28 months [4]. In agreement with previous data, we found that SAMP8 mice displayed an increased mortality compared to SAMR1 mice (Fig. 1A), and gained less weight as they aged (Fig. 1B). At six months of age, using immunohistochemistry, we did not find evidence for amyloid plaque formation in the SAMP8 compared to the SAMR1 mice using the 4G8 antibody, nor did we find pronounced differences in tau phosphorylation using antibodies 12E8, AT180, or AT8 (data not shown). However, what we found at this age was a

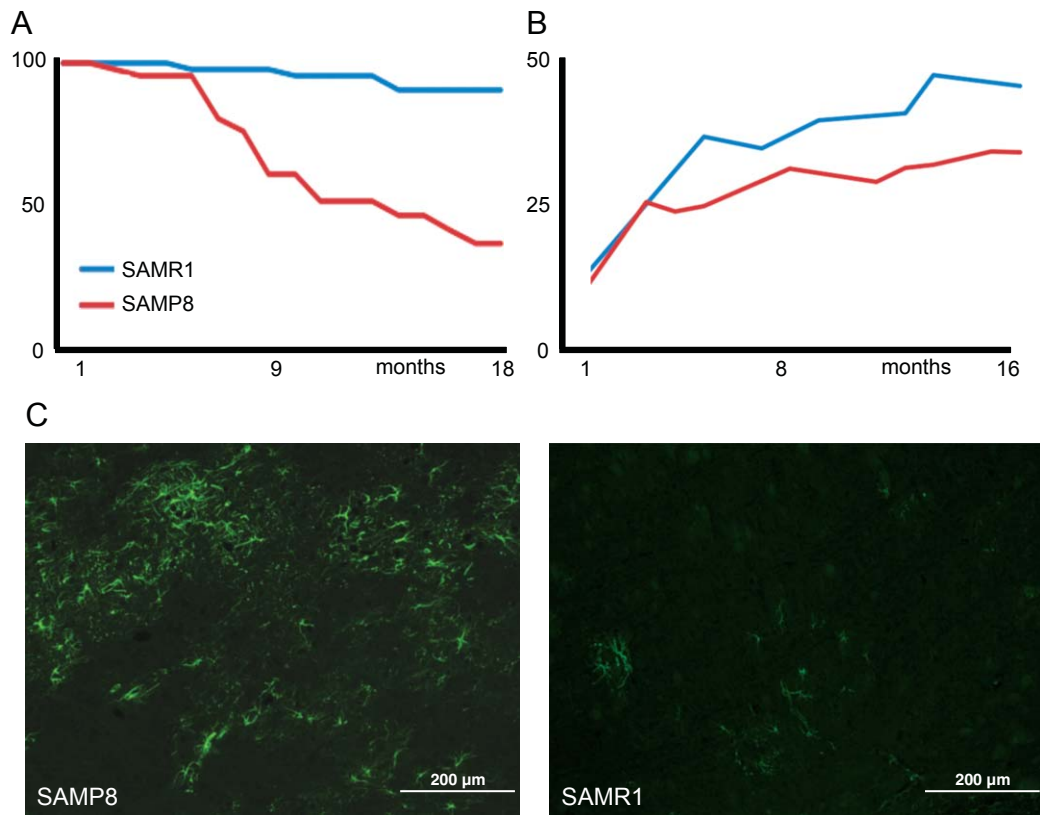


Fig. 1. Phenotypic characterization of SAMP8 mice. A) SAMP8 have an increased mortality compared to SAMR1 mice, (B) they are characterized by a reduced weight gain due to reduced body musculature, and (C) already at an age of 6 months reveal pronounced astroglial as evidenced by GFAP immunoreactivity. The pons is shown. For comparison, both strains revealed astroglial in the hippocampus but not the cortex.

pronounced astroglial in the pons of SAMP8 compared to SAMR1 mice (Fig. 1C). In the hippocampus, the two strains showed a similar degree of astroglial, while cortical areas were, in our hands, virtually free of activated astrocytes (data not shown). Phenotypically, by three to four months of age, SAMP8 mice can be discriminated from SAMR1 mice based on their reduced weight (Fig. 1B), a slightly hunched position, skin coarseness, and partial alopecia, as shown for 6 month-old mice (Fig. 2A).

Exome sequencing of SAMP8 and SAMR1 DNA

To identify genes with a putative role in the SAMP8 phenotype, we performed exome sequencing of two SAMP8 and SAMR1 mice each. Exome enrichment allowed us to successfully sequence 85–90% of the CCDS exome to a high level of coverage. From this sequencing, we found 226 SNVs that were common between the two SAMP8 mice and not seen in either SAMR1 mice or in any previous sequencing effort

(>250 exomes, mostly C57Bl/6). By removing olfactory and vomeronasal genes to eliminate a large subset of possible SNV call errors due to the high sequence homology amongst these gene family members, and excluding genes with multiple SNVs (also indicating short-read alignment errors rather than mutations) the list was reduced to 113 SNVs.

Of the 113 SNVs, 105 were selected for validation using a specific Amplifluor assay to each SNV on a larger pool of SAMP8, SAMR1, C57Bl/6, and AKR/J control samples (8 assays could not be designed with primers of sufficient quality). Of the 103 SNVs, 37 were shared with the AKR/J control strain (i.e., a polymorphism between the C57Bl/6 reference genome and the control AKR/J sample), 13 assays failed, 2 were shown to be heterozygous and unique to SAMP8, 1 was a false positive, 1 was homozygous in the SAMP8 strain and heterozygous in all controls, and 51 SNVs were unique to SAMP8 (Table 1). We found that the SNVs were found on all chromosomes but 9, 16, and Y. Most SNVs were found on chromosome 8 (a total

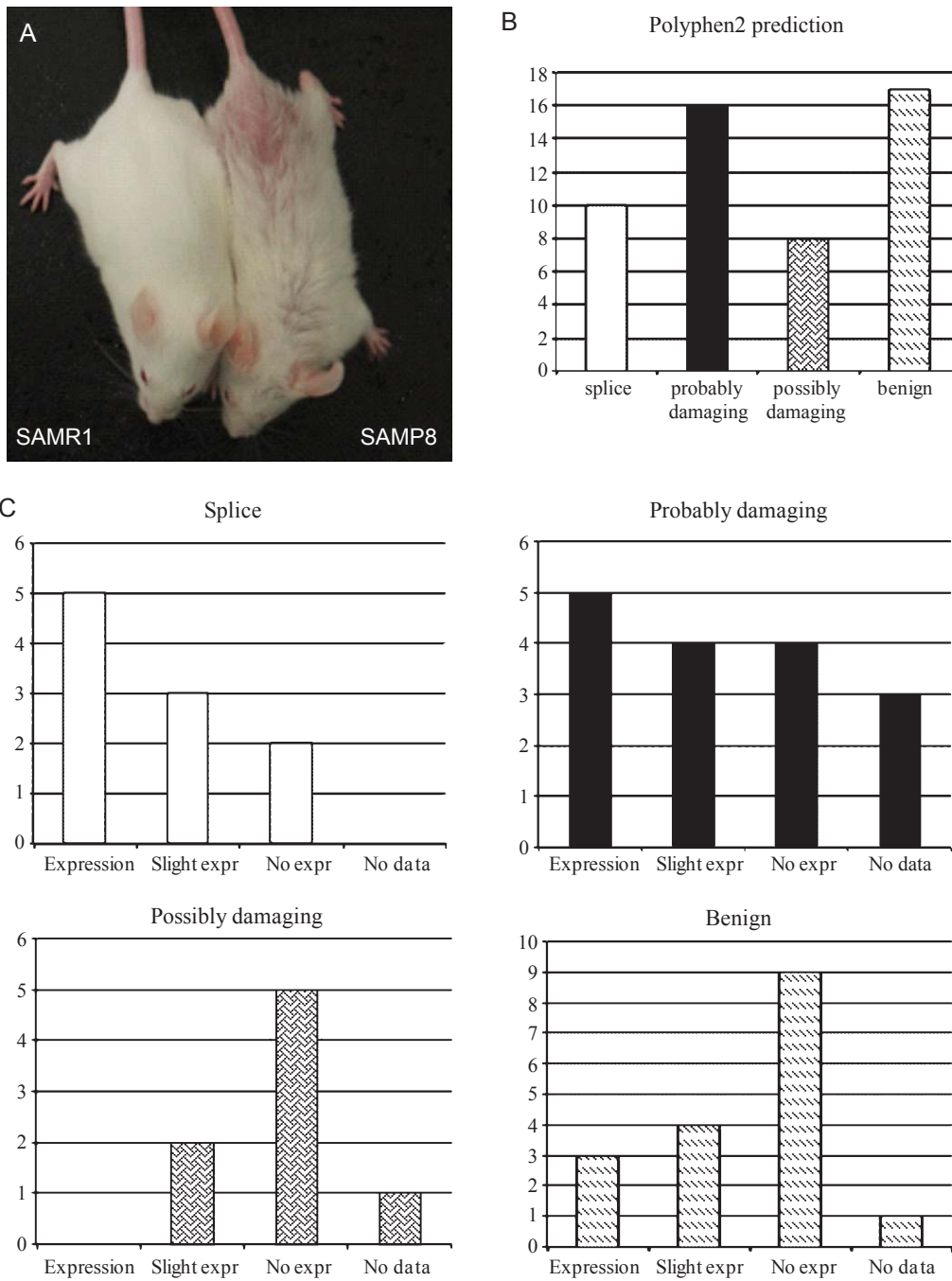


Fig. 2. Phenotype predictions. A) Partial alopecia shown for 6 month-old SAMP8 compared to SAMR1 mouse. B) Of the 51 SNVs that we identified as being unique to SAMP8, 10 are possible splice variants, while 41 are within the coding sequence. According to the amino acid substitution prediction tool Polyphen2, of the 41 coding variants, 24 are possibly or probably damaging (confidence of 0.5–1.0), while 17 are probably benign (confidence <0.5). C) By consulting the Allen brain atlas, the four groups are either moderately or strongly expressed in brain, not expressed or there are no data available.

of ten), followed by chromosome 13 (five SNVs), and 4, 7, 10, and 19 (with four SNVs each).

Polyphen prediction of SAMP8-specific single nucleotide variants and brain-specific expression of SAMP8 genes

Of the 51 SNVs that we identified as being unique to SAMP8, 10 are possible splice variants (intronic mutations located within 10 base pairs of the exon boundary), while 41 are within the coding sequence. According to the amino acid substitution prediction tool Polyphen2, of the 41 coding variants, 24 are possibly or probably damaging (confidence of 0.5–1.0), while 17 are probably benign (confidence <0.5) (Table 1, Fig. 2B). The genes with SNVs have multiple functions as suggested by a Gene Ontology (GO) analysis (Table 2).

21 of the genes have an OMIM entry and 11 have a reported phenotype in mice with a null mutation (Table 2). By consulting the Allen brain atlas (Allen Brain Atlas [Internet]. Seattle (WA): Allen Institute for Brain Science. Copyright © 2009. Available from: <http://www.brain-map.org>), we found that within the first category (splice variants), 8 of 10 genes are expressed in brain, while for 2 no expression was reported (Table 3, Fig. 2C). For the second category (probably damaging SNVs), for three genes, no data are available, four are not expressed in brain, and nine are expressed in brain, ranging from very slight to high expression levels, and from a restricted expression pattern to expression throughout the brain (Fig. 2C). For the third category (possibly damaging), no data is available for one gene; and 7 genes are listed as being expressed in brain. For the fourth category (benign), for 1 no data are available on brain expression, 5 are not expressed in brain, and 2 are slightly expressed in brain (Fig. 2C). Overall, the data indicate that at least 50% of all identified genes may have a function in the brain (Fig. 2). Whether the SNVs cause changes in levels of the encoded proteins, in their subcellular localization, association with other proteins and/or in their activity, remains to be determined in subsequent studies.

DISCUSSION

Characterized by a range of age-associated impairments, which includes the nervous system, senescence-accelerated SAMP8 mice present themselves as an excellent geriatric model [38]. We confirmed that SAMP8 mice die prematurely and that they display a reduced weight gain compared to SAMR1 mice.

Astrogliosis has been suggested as a useful marker to discriminate, at a pre-symptomatic age, the two strains; however, we found this less reliable as in our studies astrogliosis depended on the brain area investigated, with both strains showing a similar degree of activation in the hippocampus, while SAMR1 mice showed a much lesser degree of astrogliosis in the pons compared to SAMP8 mice.

We also performed exome sequencing and identified 51 SNVs (mutations) that are unique to SAMP8 mice, using senescence-resistant SAMR1 mice as well as the two inbred strains C57Bl/6 and AKR/J (from which SAMR1 and SAMP8 have been originally derived [5]) as controls. 10 of the SNVs are possible splice variants; 41 are within the coding sequence. Using the prediction tool Polyphen2, we identified 24 of the 51 SNVs as being either probably or possibly damaging. In coming up with these predictions, it is not only the type of amino acid that is critical but also where it sits in relation to the different domains, such as binding and active sites. Interestingly, not all A-T SNVs are benign, as is the case, e.g., for SLC12A4.

As evidenced by GO analysis, the mutated genes encode proteins with a wide range of cellular functions. These include ion transport, cytokine activity, axonogenesis, heme binding, GTP binding, protein transport, and others. 21 of the genes have an OMIM entry and 11 have a reported phenotype in mice with a null mutation. Consulting the Allen brain atlas revealed that a significant fraction is expressed in the brain, often with a regional pattern and ranging from very low to pronounced expression levels. Overall, the data indicate that at least 50% of all identified genes have a function in the brain.

When we analyzed the genes with brain expression in more detail and restricted the analysis to those SAMP8 SNVs for which the Polyphen tool either made no predictions or predicted that they are ‘probably or possibly damaging’, we identified several gene products that are worth being discussed in the context of the known SAMP8 brain phenotype: APBA3 (also known as Mint3) encodes an adapter protein that is part of the X11 protein family. Interestingly, APBA3 interacts with A β PP from which A β is derived by proteolytic cleavage. More recently APBA3 has been identified as a mediator of A β PP signaling: Its interaction with a set of transcriptional co-activators was shown to lead to nuclear localization and transactivation, whereas an interaction of the same set with Mint1 or Mint2 prevented nuclear localization and transactivation [39]. There is increasing evidence that in AD gene regulatory networks are deregulated [40]: In the current

Table 1

SAMP8-specific mutations and Polyphen predictions. Exome sequencing identified 51 SNVs in the genes indicated that are unique to SAMP8. Mutations were found on all chromosomes (chr) but 9, 16, and Y. Coord (coordinate); snp_id (SNP ID); ref b (nucleotide on B6 background); var b (nucleotide variant in SAMP8); aa change (amino acid change caused by variant); Polyphen prediction (such as: probably damaging); Polyph. score (Polyphen score: confidence of 0.5–1.0 for probably damaging); snp exon type (splice versus coding variants); ens name (Ensemble Gene identifier; ENSMUSG = mouse gene); ccds name (consensus coding sequence set).

Gene name	chr	coord	snp_id	ref b	var b	aa change	Polyphen prediction	Polyph. score	snp exon type	ens name	ccds name
SYT11	3	88565645	3T88565645	C	T	N/A	N/A	N/A	SPLICE	ENSMUSG00000068923	CCDS38484
ARFIP2	7	112786848	7A112786848	G	A	N/A	N/A	N/A	SPLICE	ENSMUSG00000030881	CCDS21656
TPP1	7	112895447	7T112895447	C	T	N/A	N/A	N/A	SPLICE	ENSMUSG00000030894	CCDS21661
NAE1	8	107054400	8C107054400	T	C	N/A	N/A	N/A	SPLICE	ENSMUSG00000031878	CCDS40452
TMEM208	8	107850365	8T107850365	C	T	N/A	N/A	N/A	SPLICE	ENSMUSG00000014856	CCDS22599
EDC4	8	108405065	8G108405065	C	G	N/A	N/A	N/A	SPLICE	ENSMUSG00000036270	CCDS52662
CNTNAP4	8	115305415	8T115305415	C	T	N/A	N/A	N/A	SPLICE	ENSMUSG00000031772	CCDS40482
PARP8	13	117727545	13C117727545	G	C	N/A	N/A	N/A	SPLICE	ENSMUSG00000021725	CCDS36790
6720463M24RIK	14	99467789	14G99467789	T	G	N/A	N/A	N/A	SPLICE	ENSMUSG00000022070	CCDS27309
KLF12	14	100386793	14A100386793	G	A	N/A	N/A	N/A	SPLICE	ENSMUSG00000072294	CCDS36998
SLC12A4	8	108475720	8T108475720	C	T	A->T	probably damaging	1	NON-SYN	ENSMUSG00000017765	CCDS22623
APBA3	10	80733977	10C80733977	G	C	D->H	probably damaging	1	NON-SYN	ENSMUSG00000004931	CCDS24050
PQLC3	12	17000350	12C17000350	A	C	S->R	probably damaging	1	NON-SYN	ENSMUSG00000045679	CCDS49032,CCDS25824
TMEM55B	14	51547625	14A51547625	G	A	R->W	probably damaging	1	NON-SYN	ENSMUSG00000035953	CCDS27028
D15ERTD621E	15	58274396	15T58274396	C	T	P->S	probably damaging	1	NON-SYN	ENSMUSG00000037119	CCDS37080
DNAHC8	17	30944165	17G30944165	A	G	D->G	probably damaging	1	NON-SYN	ENSMUSG00000033826	CCDS37541
F830016B08RIK	18	60459876	18A60459876	G	A	D->N	probably damaging	1	NON-SYN	ENSMUSG00000090942	CCDS50297
FXN	19	24355043	19T24355043	C	T	G->R	probably damaging	1	NON-SYN	ENSMUSG00000059363	CCDS29711
PTPRD	4	75590897	4T75590897	C	T	E->K	probably damaging	0.999	NON-SYN	ENSMUSG00000028399	CCDS18289
SPCS2	7	106993250	7T106993250	C	T	D->N	probably damaging	0.999	NON-SYN	ENSMUSG00000035227	CCDS40033
IRS2	8	11006858	8A11006858	G	A	P->S	probably damaging	0.999	NON-SYN	ENSMUSG00000038894	CCDS52477
ODZ2	11	35920361	11A35920361	C	A	C->F	probably damaging	0.999	NON-SYN	ENSMUSG00000049336	CCDS24546
HBB-BH2	7	110988898	7A110988898	G	A	T->M	probably damaging	0.997	NON-SYN	ENSMUSG00000078621	CCDS52340
ANKRD2	19	42114907	19A42114907	G	A	G->R	probably damaging	0.997	NON-SYN	ENSMUSG00000025172	CCDS50437
4930506M07RIK	19	59049495	19A59049495	G	A	T->M	probably damaging	0.977	NON-SYN	ENSMUSG00000041362	CCDS50481
TESK1	4	43456467	4T43456467	G	T	C->F	probably damaging	0.975	NON-SYN	ENSMUSG00000028458	CCDS18094
D630023F18RIK	1	65163738	1A65163738	C	A	E->D	possibly damaging	0.946	NON-SYN	ENSMUSG00000044816	CCDS15015
PRL8A9	13	27650078	13C27650078	T	C	Y->C	possibly damaging	0.933	NON-SYN	ENSMUSG00000006490	CCDS26400
PCDH7	5	58111277	5A58111277	G	A	V->M	possibly damaging	0.899	NON-SYN	ENSMUSG00000029108	CCDS19296,CCDS51505
IFNA2	4	88329388	4A88329388	G	A	A->V	possibly damaging	0.852	NON-SYN	ENSMUSG00000078354	CCDS18326
ARHGEF5	6	43238765	6A43238765	G	A	V->I	possibly damaging	0.776	NON-SYN	ENSMUSG00000033542	CCDS51759
LRRC20	10	60945213	10T60945213	G	T	S->I	possibly damaging	0.707	NON-SYN	ENSMUSG00000037151	CCDS23881
ZC3H12D	10	7587218	10T7587218	C	T	P->L	possibly damaging	0.564	NON-SYN	ENSMUSG00000039981	CCDS48496
1700019N19RIK	19	58860749	19T58860749	G	T	Q->K	possibly damaging	0.55	NON-SYN	ENSMUSG00000026931	CCDS38031

Table 1
(Continued)

Gene name	chr	coord	snp_id	ref b	var b	aa change	Polyphen prediction	Polyph. score	snp exon type	ens name	ccds name
ZFP352	4	89890773	4T89890773	C	T	T->I	benign	0.417	NON-SYN	ENSMUSG00000070902	CCDS18353
LNX1	5	75023400	5A75023400	T	A	N->Y	benign	0.355	NON-SYN	ENSMUSG00000029228	CCDS51524,CCDS51522, CCDS19347,CCDS51523
CDHR2	13	54827683	13G54827683	A	G	T->A	benign	0.291	NON-SYN	ENSMUSG00000034918	CCDS36669
LOXHD1	18	77668681	18A77668681	G	A	V->I	benign	0.239	NON-SYN	ENSMUSG00000032818	CCDS50326
GAS8	8	126048115	8T126048115	G	T	M->I	benign	0.012	NON-SYN	ENSMUSG00000040220	CCDS40512
CAR7	8	107071592	8G107071592	T	G	S->A	benign	0.01	NON-SYN	ENSMUSG00000031883	CCDS22581
F12	13	55524089	13T55524089	G	T	H->N	benign	0.01	NON-SYN	ENSMUSG00000021492	CCDS36675
BANK1	3	135897677	3C135897677	T	C	I->V	benign	0.006	NON-SYN	ENSMUSG00000037922	CCDS38645
JARID2	13	44997781	13A44997781	C	A	H->N	benign	0.002	NON-SYN	ENSMUSG00000038518	CCDS36646
BCAP31	X	70931915	XA70931915	G	A	S->L	benign	0.002	NON-SYN	ENSMUSG0000002015	CCDS30209
NLGN3	X	98502446	XA98502446	G	A	A->T	benign	0.002	NON-SYN	ENSMUSG00000031302	CCDS30313
WDR19	5	65616584	5A65616584	G	A	A->T	benign	0.001	NON-SYN	ENSMUSG00000037890	CCDS51509
CES2G	8	107487837	8T107487837	C	T	P->S	benign	0.001	NON-SYN	ENSMUSG00000031877	CCDS22589
PROM2	2	127364067	2A127364067	G	A	T->M	benign	0	NON-SYN	ENSMUSG00000027376	CCDS16704,CCDS50704
CALU	6	29311393	6T29311393	G	T	E->D	benign	0	NON-SYN	ENSMUSG00000029767	CCDS19958,CCDS19957
PDP2	8	107117577	8G107117577	T	G	C->G	benign	0	NON-SYN	ENSMUSG00000048371	CCDS22582
TBC1D30	10	120704059	10T120704059	G	T	T->N	benign	0	NON-SYN	ENSMUSG00000052302	CCDS48704

Table 2

SAMP8-specific mutations and gene descriptions. For the 51 SNVs that are unique to SAMP8 the genes are indicated, the UniProt (Universal Protein resource) name, the name of the human ortholog (homolog, where known), the OMIM entry (Online Mendelian Inheritance in Man, where available), as well as a description of the gene

Gene name	Uniprot name	Homolog	Omim	Gene description
SYT11	D3YWW9, Q9RON3	SYT11	NO_OMIM	synaptotagmin XI [Source: MGI Symbol; Acc: MGI: 1859547]
ARFIP2	Q8K221	ARFIP2	NO_OMIM	ADP-ribosylation factor interacting protein 2 [Source: MGI Symbol; Acc: MGI: 1924182]
TPP1	O89023	TPP1	http://omim.org/entry/607998	tripeptidyl peptidase I [Source: MGI Symbol; Acc: MGI:1336194]
NAE1	Q8VBW6	NAE1	http://omim.org/entry/603385	NEDD8 activating enzyme E1 subunit 1 [Source: MGI Symbol; Acc: MGI: 2384561]
TMEM208	Q9CR96	TMEM208	NO_OMIM	transmembrane protein 208 [Source: MGI Symbol; Acc: MGI: 1913570]
EDC4	Q3UJB9	EDC4	NO_OMIM	enhancer of mRNA decapping 4 [Source: MGI Symbol; Acc: MGI: 2446249]
CNTNAP4	D3YWB9, Q8BPP6, Q99P47	CNTNAP4	NO_OMIM	contactin associated protein-like 4 [Source: MGI Symbol; Acc: MGI: 2183572]
PARP8	Q3UD82	PARP8	NO_OMIM	poly (ADP-ribose) polymerase family, member 8 [Source: MGI Symbol; Acc: MGI: 1098713]
6720463M24RIK	Q8BS90	BORA	NO_OMIM	RIKEN cDNA 6720463M24 gene [Source: MGI Symbol; Acc: MGI: 1924994]
KLF12	O35738	KLF12	http://omim.org/entry/607531	Kruppel-like factor 12 [Source: MGI Symbol; Acc: MGI: 1333796]
SLC12A4	Q9JIS8	SLC12A4	http://omim.org/entry/604119	solute carrier family 12, member 4 [Source: MGI Symbol; Acc: MGI: 1309465]
APBA3	O88888	APBA3	NO_OMIM	amyloid beta (A4) precursor protein-binding, family A, member 3 [Source: MGI Symbol; Acc: MGI: 1888527]
PQLC3	Q8C6U2	PQLC3	NO_OMIM	PQ loop repeat containing [Source: MGI Symbol; Acc: MGI: 2444067]
TMEM55B	Q3TWL2	TMEM55B	NO_OMIM	transmembrane protein 55b [Source: MGI Symbol; Acc: MGI: 2448501]
D15ERTD621E	Q3UVG3	FAM91A1	NO_OMIM	DNA segment, Chr 15, ERATO Doi 621, expressed [Source: MGI Symbol; Acc: MGI: 1277178]
DNAHC8	Q91XQ0	DNAHC8	NO_OMIM	dynein, axonemal, heavy chain 8 [Source: MGI Symbol; Acc: MGI: 107714]
F830016B08RIK	NO_UNIPROT	NO_HOMOLOG	NO_OMIM	RIKEN cDNA F830016B08 gene [Source: MGI Symbol; Acc: MGI: 3588218]
FXN	O35943	FXN	http://omim.org/entry/606829	frataxin [Source: MGI Symbol; Acc: MGI: 1096879]
PTPRD	E9PVW8,E9Q7I7, E9QM93,E9QQ27, F7C4P7,Q8VBV0	PTPRD	http://omim.org/entry/601598	protein tyrosine phosphatase, receptor type, D [Source: MGI Symbol; Acc: MGI: 97812]
SPCS2	Q9CYN2	SPCS2	NO_OMIM	signal peptidase complex subunit 2 homolog (S. cerevisiae) [Source: MGI Symbol; Acc: MGI: 1913874]
IRS2	P81122	IRS2	http://omim.org/entry/600797	insulin receptor substrate 2 [Source: MGI Symbol; Acc: MGI: 109334]
ODZ2	Q9WTS5	ODZ2	NO_OMIM	odd Oz/ten-m homolog 2 (Drosophila) [Source: MGI Symbol; Acc: MGI: 1345184]
HBB-BH2	B2RVB7	HBD	NO_OMIM	hemoglobin beta, bh2 [Source: MGI Symbol; Acc: MGI: 96025]
ANKRD2	Q9WV06	ANKRD2	http://omim.org/entry/610734	ankyrin repeat domain 2 (stretch responsive muscle) [Source: MGI Symbol; Acc: MGI: 1861447]
4930506M07RIK	Q8K2Q9	KIAA1598	NO_OMIM	RIKEN cDNA 4930506M07 gene [Source: MGI Symbol; Acc: MGI: 1918903]
TESK1	O70146	TESK1	http://omim.org/entry/601782	testis specific protein kinase 1 [Source: MGI Symbol; Acc: MGI: 1201675]
D630023F18RIK	Q8C3M9	NO_HOMOLOG	NO_OMIM	RIKEN cDNA D630023F18 gene [Source: MGI Symbol; Acc: MGI: 2138198]
PRL8A9	Q9CQ58	NO_HOMOLOG	NO_OMIM	prolactin family8, subfamily a, member 9 [Source: MGI Symbol; Acc: MGI: 1914560]
PCDH7	A2RS43,E9Q2S0	PCDH7	http://omim.org/entry/602988	protocadherin 7 [Source: MGI Symbol; Acc: MGI: 1860487]
IFNA2	B1AYH7	NO_HOMOLOG	http://omim.org/entry/147562	interferon alpha 2 [Source: MGI Symbol; Acc: MGI: 107666]
ARHGEF5	E9Q7D5	NO_HOMOLOG	http://omim.org/entry/600888	Rho guanine nucleotide exchange factor (GEF) 5 [Source: MGI Symbol; Acc: MGI: 1858952]
LRRC20	Q8CI70	LRRC20	NO_OMIM	leucine rich repeat containing 20 [Source: MGI Symbol; Acc: MGI: 2387182]
ZC3H12D	E9Q3F1,E9QNR7	ZC3H12D	http://omim.org/entry/611106	zinc finger CCCH type containing 12D [Source: MGI Symbol; Acc: MGI: 3045313]
1700019N19RIK	Q9CQT6	C10ORF82	NO_OMIM	RIKEN cDNA 1700019N19 gene [Source: MGI Symbol; Acc: MGI: 1914757]

Table 2
(Continued)

Gene name	Uniprot name	Homolog	Omim	Gene description
ZFP352	A2AML7,Q8VI41	NO_HOMOLOG	NO_OMIM	zinc finger protein 352 [Source: MGI Symbol; Acc: MGI: 2387418]
LNX1	O70263	LNX1	http://omim.org/entry/609732	ligand of numb-protein X 1 [Source: MGI Symbol; Acc: MGI: 1278335]
CDHR2	E9Q7P9	CDHR2	NO_OMIM	cadherin-related family member 2 [Source: MGI Symbol; Acc: MGI: 2687323]
LOXHD1	C8YR32	LOXHD1	http://omim.org/entry/613072	lipoygenase homology domains 1 [Source: MGI Symbol; Acc: MGI: 1914609]
GAS8	Q60779	GAS8	http://omim.org/entry/605178	growth arrest specific 8 [Source: MGI Symbol; Acc: MGI: 1202386]
CAR7	Q9ERQ8	CA7	NO_OMIM	carbonic anhydrase 7 [Source: MGI Symbol; Acc: MGI: 103100]
F12	Q80YC5	F12	http://omim.org/entry/610619	coagulation factor XII (Hageman factor) [Source: MGI Symbol; Acc: MGI: 1891012]
BANK1	B0F3S4,Q14B54, Q80VH0	BANK1	http://omim.org/entry/610292	B-cell scaffold protein with ankyrin repeats 1 [Source: MGI Symbol; Acc: MGI: 2442120]
JARID2	Q62315	JARID2	NO_OMIM	jumonji, AT rich interactive domain 2 [Source: MGI Symbol; Acc: MGI: 104813]
BCAP31	A2ALM8	BCAP31	NO_OMIM	B-cell receptor-associated protein 31 [Source: MGI Symbol; Acc: MGI: 1350933]
NLGN3	A2AGI0,A2AGI2, A2AGI3,Q8BYM5	NLGN3	http://omim.org/entry/300336	neuroligin 3 [Source: MGI Symbol; Acc: MGI: 2444609]
WDR19	Q3UGF1	WDR19	http://omim.org/entry/608151	WD repeat domain 19 [Source: MGI Symbol; Acc: MGI: 2443231]
CES2G	E9PV38	NO_HOMOLOG	NO_OMIM	carboxylesterase 2G [Source: MGI Symbol; Acc: MGI: 1919611]
PROM2	Q3UUY6	PROM2	NO_OMIM	prominin 2 [Source: MGI Symbol; Acc: MGI: 2138997]
CALU	O35887	CALU	http://omim.org/entry/603420	calumenin [Source: MGI Symbol; Acc: MGI: 1097158]
PDP2	Q504M2	PDP2	NO_OMIM	pyruvate dehydrogenase phosphatase catalytic subunit 2 [Source: MGI Symbol; Acc: MGI: 1918878]
TBC1D30	Q69ZT9	TBC1D30	NO_OMIM	TBC1 domain family, member 30 [Source: MGI Symbol; Acc: MGI: 1921944]

Table 3

SAMP8-specific mutations and predictions of expression in brain. For the 51 SNVs that are unique to SAMP8 the genes are indicated we assessed the expression in brain as provided by the Allen brain atlas (Allen Brain Atlas [Internet]. Seattle (WA): Allen Institute for Brain Science. Copyright © 2009. Available from: <http://www.brain-map.org>): CTX, cortex; Hip, hippocampus; Olfact, olfactory bulb; Hypo, hypothalamus; Crb, cerebellum; Thal, thalamus; pons, pallidum, and medulla. The MGI (Mouse Genome Informatics) link provides additional information on the gene

Gene name	Expression in brain	Allen atlas link	MGI Link
SYT11	All brain	http://mouse.brain-map.org/experiment/show/2649	http://www.informatics.jax.org/marker/MGI:1859547
ARFIP2	CTX & Hip	http://mouse.brain-map.org/experiment/show/74990537	http://www.informatics.jax.org/marker/MGI:1924182
TPP1	CTX & Hip	http://mouse.brain-map.org/experiment/show/68148756	http://www.informatics.jax.org/marker/MGI:1336194
NAE1	Slight in CTX	http://mouse.brain-map.org/experiment/show/76098392	http://www.informatics.jax.org/marker/MGI:2384561
TMEM208	No expression	http://mouse.brain-map.org/experiment/show/69015745	http://www.informatics.jax.org/marker/MGI:1913570
EDC4	CTX & Hip	http://mouse.brain-map.org/experiment/show/68911011	http://www.informatics.jax.org/marker/MGI:2446249
CNTNAP4	Very slight in Hip & Olfact	http://mouse.brain-map.org/experiment/show/68196926	http://www.informatics.jax.org/marker/MGI:2183572
PARP8	CTX, Hip, & Hypo	http://mouse.brain-map.org/experiment/show/68445676	http://www.informatics.jax.org/marker/MGI:1098713
6720463M24RIK	No expression	http://mouse.brain-map.org/experiment/show/68797816	http://www.informatics.jax.org/marker/MGI:1924994
KLF12	Slight in CTX & Olfact	http://mouse.brain-map.org/experiment/show/69289279	http://www.informatics.jax.org/marker/MGI:1333796
SLC12A4	No expression	http://mouse.brain-map.org/experiment/show/69873797	http://www.informatics.jax.org/marker/MGI:1309465
APBA3	Very slight in CTX	http://mouse.brain-map.org/experiment/show/68442913	http://www.informatics.jax.org/marker/MGI:1888527
PQLC3	No data		http://www.informatics.jax.org/marker/MGI:2444067
TMEM55B	CTX, Thal, Pons, Medulla	http://mouse.brain-map.org/experiment/show/69529095	http://www.informatics.jax.org/marker/MGI:2448501
D15ERTD621E	No expression	http://mouse.brain-map.org/experiment/show/71723906	http://www.informatics.jax.org/marker/MGI:1277178
DNAHC8	No expression	http://mouse.brain-map.org/experiment/show/69626945	http://www.informatics.jax.org/marker/MGI:107714
F830016B08RIK	No data		http://www.informatics.jax.org/marker/MGI:3588218
FXN	Very high, all brain	http://mouse.brain-map.org/experiment/show/69672575	http://www.informatics.jax.org/marker/MGI:1096879
PTPRD	CTX, Hip & Thal	http://mouse.brain-map.org/experiment/show/855	http://www.informatics.jax.org/marker/MGI:97812
SPCS2	CTX, Pallidum & Hypo	http://mouse.brain-map.org/experiment/show/68667312	http://www.informatics.jax.org/marker/MGI:1913874
IRS2	Very slight in Hip & Thal	http://mouse.brain-map.org/experiment/show/71211707	http://www.informatics.jax.org/marker/MGI:109334
ODZ2	Very slight in Hip only	http://mouse.brain-map.org/experiment/show/79591631	http://www.informatics.jax.org/marker/MGI:1345184
HBB-BH2	No data		http://www.informatics.jax.org/marker/MGI:96025
ANKRD2	No expression	http://mouse.brain-map.org/experiment/show/69526647	http://www.informatics.jax.org/marker/MGI:1861447
4930506M07RIK	CTX & Hip	http://mouse.brain-map.org/experiment/show/275675	http://www.informatics.jax.org/marker/MGI:1918903
TESK1	Slight in CTX, Hip & Crb	http://mouse.brain-map.org/experiment/show/69980268	http://www.informatics.jax.org/marker/MGI:1201675
D630023F18RIK	No expression	http://mouse.brain-map.org/experiment/show/69609007	http://www.informatics.jax.org/marker/MGI:2138198
PRL8A9	No expression	http://mouse.brain-map.org/experiment/show/71656664	http://www.informatics.jax.org/marker/MGI:1914560
PCDH7	Very slight in CTX	http://mouse.brain-map.org/experiment/show/69782790	http://www.informatics.jax.org/marker/MGI:1860487

Table 3
(Continued)

Gene name	Expression in brain	Allen atlas link	MGI Link
IFNA2	No data	http://mouse.brain-map.org/experiment/show/69526838	http://www.informatics.jax.org/marker/MGI:107666
ARHGEF5	No expression	http://mouse.brain-map.org/experiment/show/69526838	http://www.informatics.jax.org/marker/MGI:1858952
LRRC20	Very slight in Crb & Olfact	http://mouse.brain-map.org/experiment/show/68797500	http://www.informatics.jax.org/marker/MGI:2387182
ZC3H12D	No expression	http://mouse.brain-map.org/experiment/show/71809097	http://www.informatics.jax.org/marker/MGI:3045313
1700019N19RIK	No expression	http://mouse.brain-map.org/experiment/show/69114465	http://www.informatics.jax.org/marker/MGI:1914757
ZFP352	No expression	http://mouse.brain-map.org/experiment/show/70785732	http://www.informatics.jax.org/marker/MGI:2387418
LNx1	No expression	http://mouse.brain-map.org/experiment/show/74277745	http://www.informatics.jax.org/marker/MGI:1278335
CDHR2	No expression	http://mouse.brain-map.org/experiment/show/69529107	http://www.informatics.jax.org/marker/MGI:2687323
LOXHD1	No expression	http://mouse.brain-map.org/experiment/show/73514737	http://www.informatics.jax.org/marker/MGI:1914609
GAS8	CTX, Hip & Thal	http://mouse.brain-map.org/experiment/show/74990538	http://www.informatics.jax.org/marker/MGI:1202386
CAR7	No expression	http://mouse.brain-map.org/experiment/show/71496276	http://www.informatics.jax.org/marker/MGI:103100
F12	No data		http://www.informatics.jax.org/marker/MGI:1891012
BANK1	Slight in CTX	http://mouse.brain-map.org/experiment/show/69528076	http://www.informatics.jax.org/marker/MGI:2442120
JARID2	Slight in olfact	http://mouse.brain-map.org/experiment/show/605	http://www.informatics.jax.org/marker/MGI:104813
BCAP31	CTX, Pons & Medulla	http://mouse.brain-map.org/experiment/show/79544798	http://www.informatics.jax.org/marker/MGI:1350933
NLGN3	High all brain	http://mouse.brain-map.org/experiment/show/70300559	http://www.informatics.jax.org/marker/MGI:2444609
WDR19	No expression	http://mouse.brain-map.org/experiment/show/70194988	http://www.informatics.jax.org/marker/MGI:2443231
CES2G	Very slight in olfact	http://mouse.brain-map.org/experiment/show/68445053	http://www.informatics.jax.org/marker/MGI:1919611
PROM2	No expression	http://mouse.brain-map.org/experiment/show/68498519	http://www.informatics.jax.org/marker/MGI:2138997
CALU	No expression	http://mouse.brain-map.org/experiment/show/69013426	http://www.informatics.jax.org/marker/MGI:1097158
PDP2	No expression	http://mouse.brain-map.org/experiment/show/70299983	http://www.informatics.jax.org/marker/MGI:1918878
TBC1D30	Very slight in CTX	http://mouse.brain-map.org/experiment/show/72283432	http://www.informatics.jax.org/marker/MGI:1921944

study, we also identified the enhancer of decapping *Ede4* [41], and *Klf12* that encodes Kruppel-like Factor 12, a member of a zinc finger protein family that regulates gene transcription [42]. Interestingly, a recent transcriptomic analysis of tau mutant mice revealed a deregulation of several transcription factors including *Zranb1* (a Zinc finger-containing protein) and *SFPQ* (splicing factor proline/glutamine rich), also known as *PSF* (Polypyrimidine tract-binding protein-associated Splicing Factor) [43]. Validation of *SFPQ* revealed that in AD the transcription factor is relocalized from the nucleus to the cytoplasm [43].

Among the genes with brain expression are several that encode enzymes such as kinases and phosphatases (*PTPRD*, *TESK1*, *TMEM55B*) that could potentially regulate the phosphorylation of cytoskeletal proteins such as tau. *TESK1* is particularly interesting as together with *Spred1*, it is an interaction partner of the kinase *MARKK/TAO1* that links the microtubule and actin cytoskeleton [44]. With a SNV in the gene encoding the signal peptidase *SPCS2*, more fundamental processes could be affected in the SAMP8 mice as depletion of *SPC3* in yeast leads to impaired secretion and the accumulation of secretory proteins [45]. *TPPI*

encodes the lysosomal enzyme tripeptidyl-peptidase 1, and mutations in this gene cause a form of spinocerebellar ataxia, with patients having a shortened lifespan. It might be possible, that the SNV found for TPP in the SAMP8 mice contributes to the shortened lifespan that characterizes the strain [46]. A SNV was also found in the FXN gene, for which a trinucleotide expansion in human causes yet another ataxia, Friedreich ataxia [47].

Finally, IRS2 (insulin receptor signaling 2) is an interesting molecule with central functions including the regulation of mammalian lifespan and nutrient homeostasis [48], glucose metabolism [49], as well as mitochondrial functions and the dealing with oxidative stress [50]. Moreover, IRS2 is a negative regulator of memory formation and has been shown to impair NMDA receptor-dependent long-term potentiation [51, 52]. All of these functions are impaired in the SAMP8 mice suggesting that an impaired IRS2 function could potentially contribute to the SAMP8 phenotype.

Having identified a total of 51 SNVs by exome sequencing that discriminate SAMP8 and SAMR1, we anticipate that these will allow a phenotypic discrimination, especially as it is evident from our list that several of the SNVs are within genes that in principal could contribute to the SAMP8 phenotype. It is reasonable to assume that a subset of the SNVs causes either changes in protein levels, stability, subcellular localization or posttranslational modification of the encoded proteins, which can be detected provided that suitable antibodies are available. The SNVs should be also useful in monitoring the SAMP8 strain to ensure that there is no genetic drift in any given colony. Furthermore, it may be possible to establish sub-lines that inherit some of the SNVs and hence result in a segregation of a subset of the phenotypic traits that affect selected systems such as the brain or the immune system.

As mentioned above, SAMP8 mice do not present with typical plaques and tangles, although the accumulation of A β and hyperphosphorylated tau has been reported [23, 26]. In order to exploit SAMP8 mice for AD research a further possibility is to cross the SAMP8 mice with either A β plaque-forming or tau tangle-forming transgenic mice. Here, for example, the question can be asked whether a tau pathology such as that of P301L tau mutant mice with a memory phenotype [53] or of K369I mutant mice with neuronal loss and a motor phenotype [54, 55] would be accelerated by the presence of distinct SAMP8 SNVs. Alternatively one could ask whether removing or reducing tau would ameliorate some of the phenotypes that charac-

terize the SAMP8 mice [56]. In conclusion, we believe that our data contribute to ascertaining SAMP8 mice as a suitable model system to study aging and dementia.

ACKNOWLEDGMENTS

This study was supported by the Estate of Dr. Clem Jones AO and by grants from the Australian Research Council and the National Health and Medical Research Council of Australia to JG, as well as the Phillip Jacoby Scholarship in Alzheimer's Dementia Research to FD. Sequencing and bioinformatic analyses were supported by the Australian Super Science Initiative funded through the Education Investment Fund to the APF.

Authors' disclosures available online (<http://www.j-alz.com/disclosures/view.php?id=1726>).

SUPPLEMENTARY MATERIAL

Supplementary material can be found here: <http://dx.doi.org/10.3233/JAD-130089>

REFERENCES

- [1] Ballard C, Gauthier S, Corbett A, Brayne C, Aarsland D, Jones E (2011) Alzheimer's disease. *Lancet* **377**, 1019-1031.
- [2] Gotz J, Ittner LM (2008) Animal models of Alzheimer's disease and frontotemporal dementia. *Nat Rev Neurosci* **9**, 532-544.
- [3] Del Valle J, Bayod S, Camins A, Beas-Zarate C, Velazquez-Zamora DA, Gonzalez-Burgos I, Pallas M (2012) Dendritic spine abnormalities in hippocampal CA1 pyramidal neurons underlying memory deficits in the SAMP8 mouse model of Alzheimer's disease. *J Alzheimers Dis* **32**, 233-240.
- [4] Pallas M, Camins A, Smith MA, Perry G, Lee HG, Casadesus G (2008) From aging to Alzheimer's disease: Unveiling "the switch" with the senescence-accelerated mouse model (SAMP8). *J Alzheimers Dis* **15**, 615-624.
- [5] Takeda T (1999) Senescence-accelerated mouse (SAM): A biogerontological resource in aging research. *Neurobiol Aging* **20**, 105-110.
- [6] Shimada A, Hasegawa-Ishii S (2011) Senescence-accelerated mice (SAMs) as a model for brain aging and immunosenescence. *Aging Dis* **2**, 414-435.
- [7] Flood JF, Morley JE (1998) Learning and memory in the SAMP8 mouse. *Neurosci Biobehav Rev* **22**, 1-20.
- [8] Cheng H, Yu J, Jiang Z, Zhang X, Liu C, Peng Y, Chen F, Qu Y, Jia Y, Tian Q, Xiao C, Chu Q, Nie K, Kan B, Hu X, Han J (2008) Acupuncture improves cognitive deficits and regulates the brain cell proliferation of SAMP8 mice. *Neurosci Lett* **432**, 111-116.
- [9] Flood JF, Farr SA, Uezu K, Morley JE (1998) Age-related changes in septal serotonergic, GABAergic and glutamatergic facilitation of retention in SAMP8 mice. *Mech Ageing Dev* **105**, 173-188.
- [10] Ikegami S, Shumiya S, Kawamura H (1992) Age-related changes in radial-arm maze learning and basal forebrain

- cholinergic systems in senescence accelerated mice (SAM). *Behav Brain Res* **51**, 15-22.
- [11] Chen GH, Wang YJ, Wang XM, Zhou JN (2004) Accelerated senescence prone mouse-8 shows early onset of deficits in spatial learning and memory in the radial six-arm water maze. *Physiol Behav* **82**, 883-890.
- [12] McGaugh JL (1966) Time-dependent processes in memory storage. *Science* **153**, 1351-1358.
- [13] Senechal Y, Kelly PH, Dev KK (2008) Amyloid precursor protein knockout mice show age-dependent deficits in passive avoidance learning. *Behav Brain Res* **186**, 126-132.
- [14] Miyamoto M (1994) [Experimental techniques for developing new drugs acting on dementia (8)–Characteristics of behavioral disorders in senescence-accelerated mouse (SAMP8): Possible animal model for dementia]. *Nihon Shinkei Seishin Yakurigaku Zasshi* **14**, 323-335.
- [15] Miyamoto M (1997) Characteristics of age-related behavioral changes in senescence-accelerated mouse SAMP8 and SAMP10. *Exp Gerontol* **32**, 139-148.
- [16] Schmitt K, Grimm A, Kazmierczak A, Strosznajder JB, Gotz J, Eckert A (2012) Insights into mitochondrial dysfunction: Aging, amyloid-beta, and tau-A deleterious trio. *Antioxid Redox Signal* **16**, 1456-1466.
- [17] Kurokawa T, Asada S, Nishitani S, Hazeki O (2001) Age-related changes in manganese superoxide dismutase activity in the cerebral cortex of senescence-accelerated prone and resistant mouse. *Neurosci Lett* **298**, 135-138.
- [18] Sato E, Oda N, Ozaki N, Hashimoto S, Kurokawa T, Ishibashi S (1996) Early and transient increase in oxidative stress in the cerebral cortex of senescence-accelerated mouse. *Mech Ageing Dev* **86**, 105-114.
- [19] Okatani Y, Wakatsuki A, Reiter RJ, Miyahara Y (2002) Melatonin reduces oxidative damage of neural lipids and proteins in senescence-accelerated mouse. *Neurobiol Aging* **23**, 639-644.
- [20] Yasui F, Ishibashi M, Matsugo S, Kojo S, Oomura Y, Sasaki K (2003) Brain lipid hydroperoxide level increases in senescence-accelerated mice at an early age. *Neurosci Lett* **350**, 66-68.
- [21] Kurokawa T, Sato E, Inoue A, Ishibashi S (1996) Evidence that glucose metabolism is decreased in the cerebrum of aged female senescence-accelerated mouse; possible involvement of a low hexokinase activity. *Neurosci Lett* **214**, 45-48.
- [22] Kitamura Y, Zhao XH, Ohnuki T, Nomura Y (1989) Ligand-binding characteristics of [3H]QNB, [3H]prazosin, [3H]rauwolscine, [3H]TCP and [3H]nitrendipine to cerebral cortical and hippocampal membranes of senescence accelerated mouse. *Neurosci Lett* **106**, 334-338.
- [23] Canudas AM, Gutierrez-Cuesta J, Rodriguez MI, Acuna-Castroviejo D, Sureda FX, Camins A, Pallas M (2005) Hyperphosphorylation of microtubule-associated protein tau in senescence-accelerated mouse (SAM). *Mech Ageing Dev* **126**, 1300-1304.
- [24] Gotz J, Gladbach A, Pennanen L, van Eersel J, Schild A, David D, Ittner LM (2010) Animal models reveal role for tau phosphorylation in human disease. *Biochim Biophys Acta* **1802**, 860-871.
- [25] Gutierrez-Cuesta J, Sureda FX, Romeu M, Canudas AM, Caballero B, Coto-Montes A, Camins A, Pallas M (2007) Chronic administration of melatonin reduces cerebral injury biomarkers in SAMP8. *J Pineal Res* **42**, 394-402.
- [26] Takemura M, Nakamura S, Akiguchi I, Ueno M, Oka N, Ishikawa S, Shimada A, Kimura J, Takeda T (1993) Beta/A4 proteinlike immunoreactive granular structures in the brain of senescence-accelerated mouse. *Am J Pathol* **142**, 1887-1897.
- [27] Fukunari A, Kato A, Sakai Y, Yoshimoto T, Ishiura S, Suzuki K, Nakajima T (1994) Colocalization of prolyl endopeptidase and amyloid beta-peptide in brains of senescence-accelerated mouse. *Neurosci Lett* **176**, 201-204.
- [28] Kumar VB, Farr SA, Flood JF, Kamlesh V, Franko M, Banks WA, Morley JE (2000) Site-directed antisense oligonucleotide decreases the expression of amyloid precursor protein and reverses deficits in learning and memory in aged SAMP8 mice. *Peptides* **21**, 1769-1775.
- [29] Morley JE, Kumar VB, Bernardo AE, Farr SA, Uezu K, Tumosa N, Flood JF (2000) Beta-amyloid precursor polypeptide in SAMP8 mice affects learning and memory. *Peptides* **21**, 1761-1767.
- [30] Nomura Y, Yamanaka Y, Kitamura Y, Arima T, Ohnuki T, Oomura Y, Sasaki K, Nagashima K, Ihara Y (1996) Senescence-accelerated mouse. Neurochemical studies on aging. *Ann N Y Acad Sci* **786**, 410-418.
- [31] Sureda FX, Gutierrez-Cuesta J, Romeu M, Mulero M, Canudas AM, Camins A, Mallol J, Pallas M (2006) Changes in oxidative stress parameters and neurodegeneration markers in the brain of the senescence-accelerated mice SAMP-8. *Exp Gerontol* **41**, 360-367.
- [32] Andrews TD, Whittle B, Field MA, Balakishnan B, Zhang Y, Shao Y, Cho V, Kirk M, Singh M, Xia Y, Hager J, Winslade S, Sjollem G, Beutler B, Enders A, Goodnow CC (2012) Massively parallel sequencing of the mouse exome to accurately identify rare, induced mutations: An immediate source for thousands of new mouse models. *Open Biol* **2**, 120061.
- [33] Lim YA, Giese M, Shepherd C, Halliday G, Kobayashi M, Takamatsu K, Staufenbiel M, Eckert A, Gotz J (2012) Role of hippocalcin in mediating Abeta toxicity. *Biochim Biophys Acta* **1822**, 1247-1257.
- [34] Li H, Durbin R (2009) Fast and accurate short read alignment with Burrows-Wheeler transform. *Bioinformatics* **25**, 1754-1760.
- [35] Li H, Handsaker B, Wysoker A, Fennell T, Ruan J, Homer N, Marth G, Abecasis G, Durbin R (2009) The Sequence Alignment/Map format and SAMtools. *Bioinformatics* **25**, 2078-2079.
- [36] Wang K, Li M, Hakonarson H (2010) ANNOVAR: Functional annotation of genetic variants from high-throughput sequencing data. *Nucleic Acids Res* **38**, e164.
- [37] Adzhubei IA, Schmidt S, Peshkin L, Ramensky VE, Gerasimova A, Bork P, Kondrashov AS, Sunyaev SR (2010) A method and server for predicting damaging missense mutations. *Nat Methods* **7**, 248-249.
- [38] Morley JE, Armbrrecht HJ, Farr SA, Kumar VB (2012) The senescence accelerated mouse (SAMP8) as a model for oxidative stress and Alzheimer's disease. *Biochim Biophys Acta* **1822**, 650-656.
- [39] Swistowski A, Zhang Q, Orcholski ME, Crippen D, Vitelli C, Kurakin A, Bredezen DE (2009) Novel mediators of amyloid precursor protein signaling. *J Neurosci* **29**, 15703-15712.
- [40] Schonrock N, Matamales M, Ittner LM, Gotz J (2011) MicroRNA networks surrounding APP and amyloid-beta metabolism - Implications for Alzheimer's disease. *Exp Neurol* **235**, 447-454.
- [41] Glasmacher E, Hoefig KP, Vogel KU, Rath N, Du L, Wolf C, Kremmer E, Wang X, Heissmeyer V (2010) Roquin binds inducible costimulator mRNA and effectors of mRNA decay to induce microRNA-independent post-transcriptional repression. *Nat Immunol* **11**, 725-733.
- [42] Ko JL, Liu HC, Loh HH (2003) Role of an AP-2-like element in transcriptional regulation of mouse mu-opioid receptor gene. *Brain Res Mol Brain Res* **112**, 153-162.

- [43] Ke Y, Dramiga J, Schutz U, Kril JJ, Ittner LM, Schroder H, Gotz J (2012) Tau-mediated nuclear depletion and cytoplasmic accumulation of SFPQ in Alzheimer's and Pick's disease. *PLoS One* **7**, e35678.
- [44] Johne C, Matenia D, Li XY, Timm T, Balusamy K, Mandelkow EM (2008) Spred1 and TESK1—two new interaction partners of the kinase MARKK/TAO1 that link the microtubule and actin cytoskeleton. *Mol Biol Cell* **19**, 1391-1403.
- [45] Meyer HA, Hartmann E (1997) The yeast SPC22/23 homolog Spc3p is essential for signal peptidase activity. *J Biol Chem* **272**, 13159-13164.
- [46] Sun Y, Almomani R, Breedveld GJ, Santen GW, Aten E, Lefeber DJ, Hoff JJ, Brusse E, Verheijen FW, Verdijk RM, Kriek M, Oostra B, Breuning MH, Losekoot M, den Dunnen JT, van de Warrenburg BP, Maat-Kievit AJ (2013) Autosomal recessive spinocerebellar ataxia 7 (SCAR7) is caused by variants in TPP1, the gene involved in classic late-infantile neuronal ceroid lipofuscinosis 2 disease (CLN2 Disease). *Hum Mutat* **34**, 706-713.
- [47] Delatycki MB, Corben LA (2012) Clinical features of Friedreich ataxia. *J Child Neurol* **27**, 1133-1137.
- [48] Taguchi A, Wartschow LM, White MF (2007) Brain IRS2 signaling coordinates life span and nutrient homeostasis. *Science* **317**, 369-372.
- [49] Choudhury AI, Heffron H, Smith MA, Al-Qassab H, Xu AW, Selman C, Simmgen M, Clements M, Claret M, Maccoll G, Bedford DC, Hisadome K, Diakonov I, Moosajee V, Bell JD, Speakman JR, Batterham RL, Barsh GS, Ashford ML, Withers DJ (2005) The role of insulin receptor substrate 2 in hypothalamic and beta cell function. *J Clin Invest* **115**, 940-950.
- [50] Sadagurski M, Cheng Z, Rozzo A, Palazzolo I, Kelley GR, Dong X, Krainc D, White MF (2011) IRS2 increases mitochondrial dysfunction and oxidative stress in a mouse model of Huntington disease. *J Clin Invest* **121**, 4070-4081.
- [51] Martin ED, Sanchez-Perez A, Trejo JL, Martin-Aldana JA, Cano Jaimez M, Pons S, Acosta Umanzor C, Menes L, White MF, Burks DJ (2012) IRS-2 Deficiency impairs NMDA receptor-dependent long-term potentiation. *Cereb Cortex* **22**, 1717-1727.
- [52] Irvine EE, Drinkwater L, Radwanska K, Al-Qassab H, Smith MA, O'Brien M, Kielar C, Choudhury AI, Krauss S, Cooper JD, Withers DJ, Giese KP (2011) Insulin receptor substrate 2 is a negative regulator of memory formation. *Learn Mem* **18**, 375-383.
- [53] Pennanen L, Wolfer DP, Nitsch RM, Gotz J (2006) Impaired spatial reference memory and increased exploratory behavior in P301L tau transgenic mice. *Genes Brain Behav* **5**, 369-379.
- [54] Liu X, Dobbie M, Tunningley R, Whittle B, Zhang Y, Ittner LM, Gotz J (2011) ENU mutagenesis screen to establish motor phenotypes in wild-type mice and modifiers of a pre-existing motor phenotype in tau mutant mice. *J Biomed Biotechnol* **2011**, 130947.
- [55] Ittner LM, Ke YD, Gotz J (2009) Phosphorylated Tau Interacts with c-Jun N-terminal Kinase-interacting Protein 1 (JIP1) in Alzheimer Disease. *J Biol Chem* **284**, 20909-20916.
- [56] Ittner LM, Ke YD, Delerue F, Bi M, Gladbach A, van Eersel J, Wolfing H, Chieng BC, Christie MJ, Napier IA, Eckert A, Staufenbiel M, Hardeman E, Gotz J (2010) Dendritic function of tau mediates amyloid-beta toxicity in Alzheimer's disease mouse models. *Cell* **142**, 387-397.